Check for updates

EurJIC
European Journal of Inorganic Chemistry

Concept
doi.org/10.1002/ejic.202400809

Chemistry Europe
European Chemical Societies Publishing

www.eurjic.org

Does Fluorine Make a Difference? How Fluoro Groups Influence the (Structural) Properties of MOFs

Uwe Ruschewitz*[a]

Herein, the influence of fluorine substituents on the structural and physical properties of MOFs with aromatic carboxylate ligands is investigated. To achieve this, the focus is limited to a few widely used ligand classes, e.g. terephthalates or trimesates. It is shown that the torsion angle between the phenyl ring and the carboxylate groups plays a decisive role. This can also be transferred to more complex ligands. These considerations clearly show why there are isostructural variants of some MOFs with perfluorinated ligands known (e.g. MIL-53), while for others no successful synthesis has been reported up to now (e.g. HKUST-1). In order to investigate the influence of the fluorination of the linker on the properties of the corresponding MOFs, isostructural systems were analysed more specifically. It was found that the thermal and chemical stability decreases with fluorination, while the absorption of CO_2 in particular is enhanced. With regard to the specific surface area (S_{BET}), the results are contradictory.

Introduction

The year 1999, with the discovery of MOF-5[1] and HKUST-1,[2] is typically regarded as the starting point of the still ongoing high research interest in metal-organic frameworks (MOFs), even though some MOF-like compounds had already been published before 1999.[3–6] Likewise, the year 2007 with the publication of FMOF-1[7] can be regarded as the decisive milestone in the field of fluorine-containing MOFs (FMOFs), although other MOFs with fluorine-containing inorganic nodes or the readily available linker 4,4′-(hexafluoroisopropylidene)bis(benzoate) had already been reported before.[8,9] Nevertheless, the very high H_2, N_2 or O_2 gas uptake of FMOF-1, which is composed of Ag^+ cations and the linker 3,5-bis(trifluoromethyl)-1,2,4-triazolate, as well as its high hydrophobicity and stability even in boiling water, immediately attracted a great deal of attention.[10,11] Structurally, it is noteworthy that the fluorine atoms of the CF_3 groups in FMOF-1 all protrude into its pores, so that they are exposed for an optimal interaction with guests in its pores.

Numerous other FMOFs have been described since 2007. Several review articles, some of which have only recently appeared, summarise these results as well as the diverse applications of FMOFs in the fields of gas separation and storage, sensor technology (luminescence), catalysis or hydrophobicity comprehensively.[8,9,12–14] Also, the influence of the fluorine substituents on the structural properties of the resulting MOFs has already been addressed in some of these review articles.[8,9] At the beginning of our own investigations, we asked ourselves, why there are only very few FMOFs that are isostructural to known non-fluorinated representatives? If the influence of fluorine substituents on the properties of FMOFs is to be reliably determined, it is important to compare isostructural systems. As *Pachfule et al.* wrote back in 2012: "… high H_2 uptake in F-MOFs is not a universal phenomenon, but is rather system-specific and differs from system to system."[15]

In this concept paper, I would like to focus on some well-known aromatic carboxylate linkers (Scheme 1) that have been used for the construction of many, sometimes very important MOFs. For all these linkers, partial and sometimes perfluorinated derivatives are available (Scheme 1). It is the aim of this concept paper to work out the influence of fluorine substituents on the structures of the resulting MOFs and in which cases they enable the formation of isostructural MOFs and in which cases they do not. Especially in the case of isostructural "MOF pairs", the influence of fluorine on the properties of the respective MOFs will then be analysed. Due to the limited space, I will not be able to include some linkers and "MOF pairs" that are also highly interesting, such as the $BPDC^{2-}$ linker (4,4′-biphenyldicarboxylate), which is incorporated in the structure of MIL-88.[16] The perfluorinated variant of the linker leads to the coordination polymer MOFF-1 with a Cu_2 paddlewheel unit,[17] which in turn is isostructural to MOF-118 with the unfluorinated $BPDC^{2-}$ linker.[18]

Table 1 lists selected examples of MOFs constructed from the archetypal linkers and their fluorinated analogues presented in Scheme 1. The source for these MOFs is always the MOF subset[19,20] of the CSD database (March 2024, 125,383 entries).[21] It should be noted that there are other possible substitution patterns for some linkers in Scheme 1. However, only those linkers, for which MOFs were reported in the MOF subset,[19,20] have been sketched. From a basic search in the MOF subset, it can be estimated that $< 5\,\%$ of the entries belong to the FMOF subgroup.

It is the objective of this contribution to carve out possible factors for the successful synthesis of isostructural MOFs with fluorinated and non-fluorinated ligands. If attempts to synthe-

[a] *Prof. Dr. U. Ruschewitz*
Department of Chemistry and Biochemistry, University of Cologne, Greinstraße 6, 50939 Köln, Germany
E-mail: uwe.ruschewitz@uni-koeln.de

© 2025 The Author(s). European Journal of Inorganic Chemistry published by Wiley-VCH GmbH. This is an open access article under the terms of the Creative Commons Attribution License, which permits use, distribution and reproduction in any medium, provided the original work is properly cited.

© 2025 The Author(s). European Journal of Inorganic Chemistry published by Wiley-VCH GmbH

Concept
doi.org/10.1002/ejic.202400809

sise such isostructural fluorinated MOFs were unsuccessful, reasons for the formation of non-isostructural fluorinated congeners will be highlighted as well. These considerations will mainly focus on structural aspects, possible synthetic hurdles will only briefly be addressed.

Finally, for selected examples of isostructural MOFs, some properties of MOFs with and without fluorine substituents are compared in order to obtain a clear view on how fluorine affects these properties.

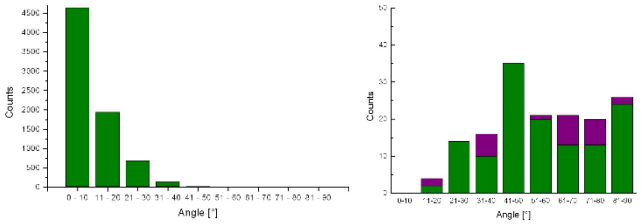

Figure 1. Torsion angles between carboxylate groups and benzene rings in coordination polymers and MOFs containing BDC^{2-} (left) and *pF*-BDC^{2-} (right) linkers. Results shown in green were extracted from the Cambridge Structural Database (CSD), results shown in violet are from ref. [55]. Reprinted (adapted) with permission from ref. [55]. Copyright 2011 American Chemical Society.

Discussion

MOFs with BDC^{2-} Linkers and their Fluorinated Derivatives

pF-BDC^{2-} is a readily available linker, and its acid can be purchased. A straightforward synthesis was published in 2010.[54] It is well-known that fluorine substituents in *ortho* position to a carboxylate group lead to a torsion of the latter. Two reasons can be given for this effect:[55–58] 1) the electron withdrawing nature of the fluorine substituent weakens the C_{phenyl}-COO^- bond and thus reduces the rotation barrier; 2) repulsion between the negatively charged oxygen atoms of the carboxylate group and the fluorine substituent leads to the observed rotation. Back in 2011, this effect was already analysed in detail (Figure 1).

Figure 1 shows that in coordination polymers and MOFs with the unfluorinated BDC^{2-} linker, the torsion angles are mainly in the range 0° to 20°, so the linker is almost planar. In compounds with *pF*-BDC^{2-}, these torsion angles are, in most cases, enhanced to 40° and more.

As a first example, MOFs with the DMOF-1[22] topology and its fluorinated congeners JAST-2 and JAST-3[27] will be discussed. They belong to the pillared-layered MOFs, i.e. Cu_2 paddlewheel units are bridged by the BDC^{2-} linkers to form grid-type layers, which are connected by neutral bifunctional N-donor ligands such as 1,4-diazabicyclo[2.2.2]octane (dabco). For a better comparison, JAST-1 will be included, which is constructed from Cu(II), unfluorinated BDC^{2-}, and dabco.[27] For JAST-1 (with BDC^{2-}) and JAST-2 (with *dF*-BDC^{2-}), torsion angles of 0° are found, whereas for JAST-3 (with *pF*-BDC^{2-}) this angle is increased to 36°. This has a significant influence on the aperture of the channels along [001], which is 7.9×7.9 $Å^2$ in JAST-1 and JAST-2, but decreases to 5.3×5.3 $Å^2$ and 6.3×6.3 $Å^2$ in JAST-3 depending on the orientation of the phenyl rings. Therefore, these phenyl rings were described as "fins" in these DMOF-1 structures.[27] The influence of the different apertures of the channels along [001] on the N_2 adsorption could not be compared, as JAST-3 was too unstable to conduct these measurements. A detailed analysis of the thermal stabilities of these MOFs was not reported. When comparing JAST-1 and JAST-2, a slight decrease of the number of N_2 molecules per pore (11.9 to 11.4) and the micropore volume (0.73 to 0.62 cm^3/g) was observed, reflecting the slightly larger spatial demand of fluorine compared to hydrogen. On the other hand, the isosteric heat of adsorption increases slightly from 15.4 to 16.8 kJ/mol.

MOFs with the MIL-53 topology show an interesting breathing effect,[23] i.e. the pores and – accordingly the unit cells – of a MOF expand or shrink in dependence of temperature, pressure or guest uptake/release. Such a breathing effect was also found in F_4-MIL-53(Al) with the *pF*-BDC^{2-} linker. In contrast to unfluorinated MIL-53(Al), this breathing is solely induced by temperature. It occurs with almost no hysteresis and fast kinetics.[29] The torsion angle between the disordered C_6F_4 phenyl ring and the carboxylate group in F_4-MIL-53(Al) is 37.1° and thus significantly increased compared to the respective angles in unfluorinated as-synthesised MIL-53(Al) (16.9° and 20.7°). The decomposition temperature decreases from 500 °C for the unfluorinated MOF to 450 °C for its perfluorinated analogue. This decreased thermal stability of FMOFs will be discussed later on in more detail. The specific surface area decreases from 1480 m^2/g to 1042 m^2/g using Argon adsorption analysis at 87 K. This was attributed to the presence of bulkier fluorine substituents in F_4-MIL-53(Al).[29] Very recently, F_4-MIL-53(Al) was incorporated in mixed matrix membranes with an enhanced butanol/water pervaporation performance.[59]

Another interesting class of flexible MOFs with a breathing behaviour are those with the MIL-88 topology; the MOFs with BDC^{2-} linkers are denominated as MIL-88B.[16] Isostructural MOFs with the perfluorinated *pF*-BDC^{2-} linker have also been published.[30,60] The unit cell volume increases slightly from 3375 $Å^3$ for MIL-88B to 3440 $Å^3$ for MIL-88B(4F).[30] This indicates a slightly higher steric demand of the fluorine substituents. This enhanced steric demand of four fluorine substituents was held

Uwe Ruschewitz received his PhD at the Technical University of Aachen (Germany). After postdoctoral studies with A. K. Cheetham at the UCSB in Santa Barbara, he returned to Aachen, where he finished his habilitation in 2000. In the same year, he was appointed as a Professor of Inorganic Chemistry at the University of Cologne. His interests are in the field of synthetic inorganic solid-state chemistry focusing on ionic carbides, MOFs with fluorinated linkers and anionic MOFs. His group has developed a strong expertise in solving and refining crystal structures from powder diffraction data.

© 2025 The Author(s). European Journal of Inorganic Chemistry published by Wiley-VCH GmbH

10990682c, 2025, 10, Downloaded from https://chemistry-europe.onlinelibrary.wiley.com/doi/10.1002/ejic.202400809 by Bibl. der Universitat zu Koln, Wiley Online Library on [19/01/2026]. See the Terms and Conditions (https://onlinelibrary.wiley.com/terms-and-conditions) on Wiley Online Library for rules of use; OA articles are governed by the applicable Creative Commons License

Concept
doi.org/10.1002/ejic.202400809

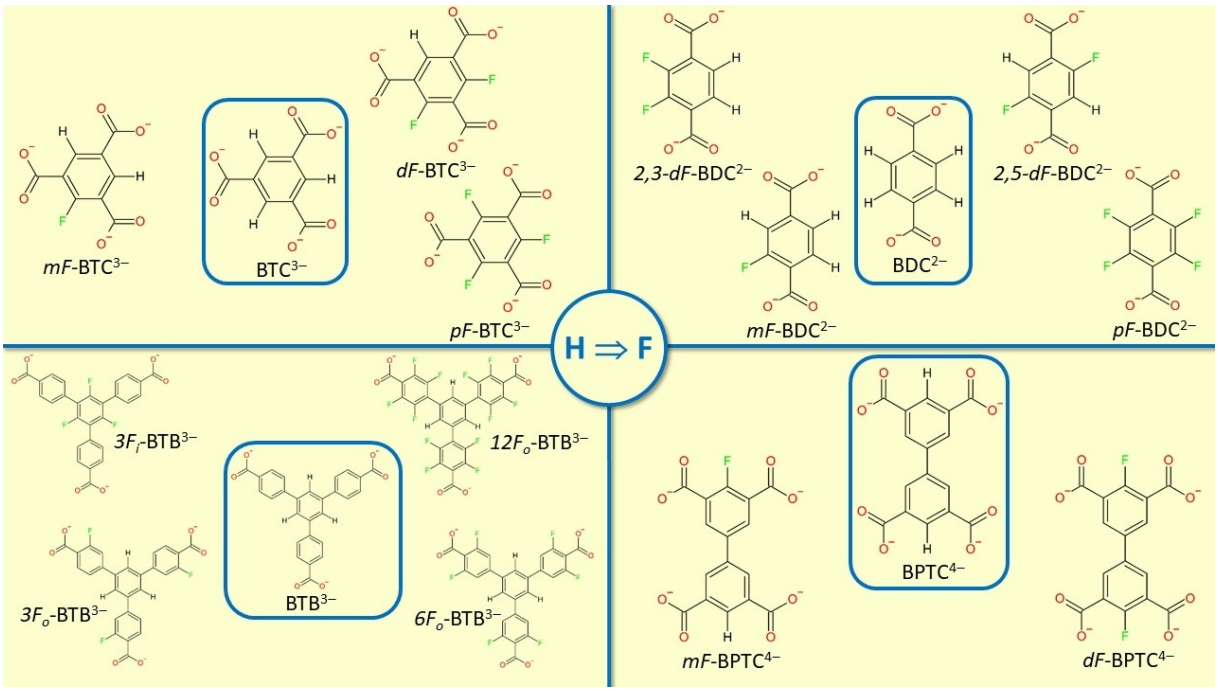

Scheme 1. Summary of the linkers discussed in this concept paper with their abbreviations; BTC^{3-}: 1,3,5-benzenetricarboxylate; BDC^{2-}: 1,4-benzenedicarboxylate; $BPTC^{4-}$: 3,3′,5,5′-biphenyltetracarboxylate; BTB^{3-}: 1,3,5-benzenetribenzoate.

Table 1. List of exemplary MOFs with the linkers presented in Scheme 1. Isostructural MOF pairs with a fluorinated and a non-fluorinated congener are highlighted in red.

Non-fluorinated			Fluorinated		
Linker	Exemplary MOFs	Entries in MOF subset[16]	Linker	Exemplary MOFs	Entries in MOF subset[16]
BDC^{2-}	DMOF-1;[22] MIL-53;[23] MIL-88B;[16] MIL-101;[24] MOF-5;[1] UiO-66[25]	3536	*mF*-BDC^{2-}	CPM-108F[26]	5
			2,3-*dF*-BDC^{2-}	JAST-2[27]	3
			2,5-*dF*-BDC^{2-}	JXNU-14[28]	1
			pF-BDC^{2-}	JAST-3;[27] F_4-MIL-53(Al);[29] MIL-88B(4F);[30] UiO-66-F4;[31] YCM-101[32]	218
BTC^{3-}	HKUST-1;[2] MIL-96;[33] MIL-100[34]	2031	*mF*-BTC^{3-}	UHM-31;[35] UHM-33;[35] UoC-7(1F)[a],[36]	19
			dF-BTC^{3-}	*dF*-UHM-33;[37] UoC-4;[38] UoC-7(2F)[a],[36]	4
			pF-BTC^{3-}	UoC-6[39]	4
$BPTC^{4-}$	MFM-300[40] ≡ InOF-1[41]	389	*mF*-$BPTC^{4-}$	UoC-1(1F);[42] UoC-2(Ga,1F);[a],[43] UoC-2(In,1F)[a],[43]	2
			dF-$BPTC^{4-}$	UoC-2(Ga,2F);[a],[43] UoC-2(In,2F)[a],[43]	0
BTB^{3-}	La-BTB;[44] MOF-177;[45] MOF-520;[46] MOF-829[47]	546	$3F_f$-BTB^{3-}	UoC-3;[48] UoC-9;[49] UoC-11[a],[50]	7
			$3F_o$-BTB^{3-}	MOF-177-H;[51] MUV-12(*o*-F_3)[b],[52]	2
			$6F_o$-BTB^{3-}	MOF-177-F[51]	5
			$12F_o$-BTB^{3-}	MOFF-4[53]	1

[a] not yet published in MOF subset; [b] also a derivative with fluorine groups in *meta* positions has been reported.

© 2025 The Author(s). European Journal of Inorganic Chemistry published by Wiley-VCH GmbH

10990682c, 2025, 10, Downloaded from https://chemistry-europe.onlinelibrary.wiley.com/doi/10.1002/ejic.202400809 by Bibl. der Universitat zu Koln, Wiley Online Library on [19/01/2026]. See the Terms and Conditions (https://onlinelibrary.wiley.com/terms-and-conditions) on Wiley Online Library for rules of use; OA articles are governed by the applicable Creative Commons License

responsible for a decreasing swelling amplitude of the breathing from 136% in MIL-88B to 54% in MIL-88B(4F) (swelling amplitude: $(V_{open}–V_{dry})/V_{dry}$).[27] The results of the gas sorption properties are inconclusive. For MIL-88B no significant N_2 uptake was reported ($S_{BET}=8$ m^2/g), as after dehydration the pores contract.[30] Similar findings were reported for MIL-88B(4 F) with $S_{BET}=32$ m^2/g.[30] However, in another work, mild activation at 50 °C leads to a Langmuir surface area of 635 m^2/g in N_2 gas sorption measurements.[60] Both MOFs decompose around 250 °C. Most important in the context of this concept paper is the fact that for both MOFs X-ray single crystal structure analyses have been published,[60,61] so that structural features can be compared in detail. In Figure 2, the BDC^{2-} linker in MIL-88B and the *pF*-BDC^{2-} linker in MIL-88B(4 F) are depicted.

As can be seen in Figure 2, the *pF*-BDC^{2-} linker is disordered over two positions in MIL-88B(4F), very similar to what was described for this linker in F_4-MIL-53(Al) (*vide supra*). As a consequence of the decreased rotation barrier around the $C_{carboxylate}$-C_{phenyl} bond due to the electron withdrawing nature of the fluoro substituents, an increased torsion angle between the carboxylate group and the C_6F_4 phenyl ring of 64.1° is observed (1.7° in MIL-88B). However, the coordination to the adjacent Fe_3O secondary building unit is completely unaffected by this tilting, since carboxylate groups in the *para* position can compensate for this torsion by rotating in the opposite direction. This illustrates nicely, why isostructural MOFs of BDC^{2-} and *pF*-BDC^{2-} are found very frequently in the literature.

Similar results were obtained for UiO-66[25] and its perfluorinated derivative UiO-66-F4.[31] The surface areas are $S_{Langmuir}=1187$ m^2/g for UiO-66 and $S_{BET}=690$ m^2/g for UiO-66-F4. In another work $S_{BET}=1525$ m^2/g for UiO-66 and $S_{BET}=833$ m^2/g for UiO-66-F4 were reported.[62] Obviously, the specific surface area decreases significantly for the perfluorinated material. Also, the decomposition temperature decreases considerably for the perfluorinated MOF.[62] The X-ray powder diffraction patterns give rise to a defect-rich crystal structure of UiO-66-F4,[31] so that a discussion of structural details is not meaningful at this point.

All these examples clearly demonstrate that MOFs with BDC^{2-} ligands should be accessible as isostructural congeners with a fluorinated or perfluorinated BDC^{2-} linker as well. To the best of our knowledge, there is one (important) example missing: a perfluorinated derivative of MOF-5, as a partially fluorinated derivative of MIL-101 has also been described.[63] In quantum chemical calculations, the properties of MOF-5(4F) have already been elucidated,[58] but a chemical synthesis and structural characterisation of this interesting MOF has still not been reported in the literature. With regard to the isoreticular chemistry developed by *Yaghi* and co-workers especially for MOFs with the MOF-5 type structure,[64] this is very surprising. Due to the disorder of the *pF*-BDC^{2-} linker found in F_4-MIL-53(Al) or MIL-88B(4F), one might expect a similar disorder in potential MOF-5(4F) leading to an interpenetrating structure as found for IRMOF-0[65] or, more likely, to a simple cubic structure with a(MOF-5(4 F)) $\approx \frac{1}{2}a$(MOF-5). However, this is speculative at the moment and needs to be verified by experiment.

MOFs with BTC^{3-} Linkers and their Fluorinated Derivatives

The situation is completely different, when going from the BDC^{2-} to the BTC^{3-} linker and its fluorinated derivatives. First of all, the accessibility of the fluorinated derivatives is more restricted. Only for *mF*-BTC^{3-}, a synthesis was published in the literature almost 70 years ago.[66] Very recently, it turned out that not the free acid H_3*mF*-BTC is obtained in this synthesis, but its monopotassium salt K[H_2*mF*-BTC].[67] Later on, the linkers with two or three fluoro substituents have also been synthesised as their monopotassium salts.[37] However, the poor availability of the starting materials especially for the synthesis of K[H_2*pF*-BTC] led to only very few examples of MOFs and coordination polymers with these linkers. Figure 3 shows the thermal stability of the monopotassium salts of the linkers H_2*mF*-BTC^-, H_2*dF*-BTC^-, and H_2*pF*-BTC^-, as determined by TGA.[37] Similar results were obtained for HKUST-1 and isostructural UHM-31 with the monofluorinated BTC^{3-} linker, where the

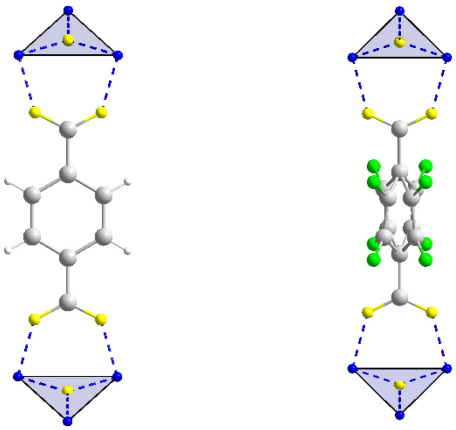

Figure 2. BDC^{2-} linker in MIL-88B (left)[61] and *pF*-BDC^{2-} linker in MIL-88B(4F) (right)[60] with its adjacent Fe_3O secondary building units (blue spheres: Fe, yellow spheres: O, green spheres: F, larger grey spheres: C, smaller white spheres: H).

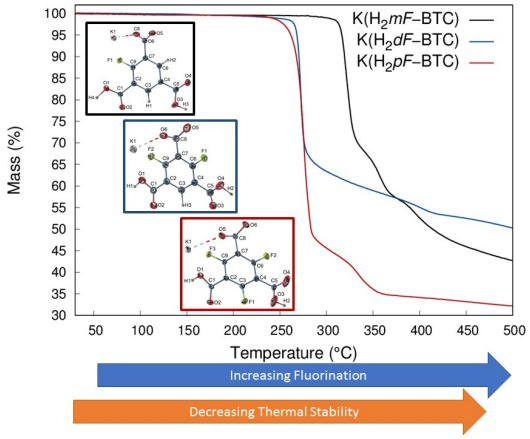

Figure 3. Thermogravimetric analyses (TGA) of the monopotassium salts of the linkers H_2*mF*-BTC^-, H_2*dF*-BTC^-, and H_2*pF*-BTC^-.[37] Reprinted (adapted) with permission from ref. [37]. Copyright 2019 American Chemical Society.

© 2025 The Author(s). European Journal of Inorganic Chemistry published by Wiley-VCH GmbH

10990682c, 2025, 10, Downloaded from https://chemistry-europe.onlinelibrary.wiley.com/doi/10.1002/ejic.202400809 by Bibl. der Universitat zu Koln, Wiley Online Library on [19/01/2026]. See the Terms and Conditions (https://onlinelibrary.wiley.com/terms-and-conditions) on Wiley Online Library for rules of use; OA articles are governed by the applicable Creative Commons License

decomposition temperature decreases from 250 °C to 220 °C for the latter.[35] For several other MOFs and CPs, a similar behaviour was reported.[37] Also the chemical stability of these compounds, e.g. their stability in water, was investigated showing comparable results: with an increasing fluorination of the linker, the chemical and thermal stabilities decrease significantly.[37] This is due to the electron withdrawing nature of the fluorine substituents, which reduces the electron density in the $C_{carboxylate}$-C_{phenyl} bond, thereby facilitating the decarboxylation of these materials, which is typically the first decomposition step of carboxylate-based MOFs and CPs.

The reduced electron density in the $C_{carboxylate}$-C_{phenyl} bond also decreases its rotation barrier, which leads to either disordered linkers, as discussed for the *pF*-BDC^{2-} linker before, or, as will be shown in the following, increased torsion angles between the phenyl ring and the carboxylate moieties. Figure 4 depicts strontium MOFs and CPs of H-BTC^{2-} and its fluorinated analogues, wherein one carboxylate group each is not deprotonated. These Sr-based MOFs and CPs[68,69] are, to the best of our knowledge, the only example of a series of compounds starting from the non-fluorinated up to the perfluorinated BTC^{3-} linker. Figure 4 also specifies the torsion angles between the phenyl ring and the carboxylate/carboxylic acid function. The mean values increase from 20° ($HBTC^{2-}$) to 22° (H*mF*-BTC^{2-}), 27.7° (H*dF*-BTC^{2-}), and 40.7° (H*pF*-BTC^{2-}). The torsion angles between the phenyl ring and the –COOH group are mainly unaffected by the fluorination, whereas the torsion angles of the carboxylate groups in *ortho* position to a fluorine substituent show a significant increase. In the compound with the H*mF*-BTC^{2-} linker (second from left, Figure 4), the fluorine substituent is disordered over two positions. Accordingly, the resulting torsion angle of the carboxylate group between these two partly occupied fluorine positions (49°) is significantly increased, when these two fluorine positions are fully occupied (60° in the H*dF*-BTC^{2-} and 58° in the H*pF*-BTC^{2-} compound). In the latter, there are two positions for carboxylate groups between two fluorine substituents in *ortho* positions, resulting in a torsion angle of 58° for both carboxylate moieties. It is thus not too surprising that with the H*pF*-BTC^{2-} linker, a 2D coordination polymer with a completely different structural arrangement is formed (cp. the coordination to Sr^{2+} cations as depicted in Figure 4), whereas with the other three linkers, similar 3D MOFs were obtained: $^3_\infty$[Sr(H-BTC)$(H_2O)_2$] $\times\frac{1}{2}$ H_2O and $^3_\infty$[Sr(H*mF*-BTC)$(H_2O)_2$]$\times\frac{1}{2}$ H_2O are isostructural ($P\bar{1}$, $Z=2$), $^3_\infty$[Sr(H*dF*-BTC)$(H_2O)_2$]$\times\frac{1}{2}$ H_2O is a 3D MOF with the same topology, but a slightly different symmetry ($C2/c$, $Z=8$). In the light of these results (also cp. Table 2), one can predict that it will not be possible to synthesize a MOF with the perfluorinated *pF*-BTC^{3-} linker isostructural to well-known HKUST-1.

In Table 2, these considerations about the torsion angle between the phenyl ring and carboxylate groups in BTC^{3-} based MOFs/CPs are expanded to other examples. They confirm the conclusions of the discussion above about the Sr-based MOFs/CPs. The torsion angles increase considerably with a larger number of fluorine substituents. Especially for carboxylate groups in *ortho* position to a fluorine substituent – and even more for a carboxylate group in-between two fluorine substituents in *ortho* positions – very large torsion angles are observed. In UoC-6 with the perfluorinated *pF*-BTC^{3-} linker and a Sc^{3+} node, two torsion angles of 81.4° with an almost perpendicular orientation were found.[39] It is, however, somewhat surprising that the third torsion angle is significantly smaller (17.8°). This indicates that the potential energy surface for the rotation is "smooth" or, in other words, the rotation barriers are not very high and the repulsive interactions not very strong. Currently, we are conducting DFT calculations on this issue to get a more quantitative picture of these rotation barriers and potential energy surfaces. Another unexpected torsion angle is observed for UoC-4, a 3D Sc-based MOF very similar to UoC-6 with the difluorinated *dF*-BTC^{3-} linker (Table 2): two perpendicular orientations (90°) of the carboxylate groups and one coplanar orientation (0°) with respect to the phenyl

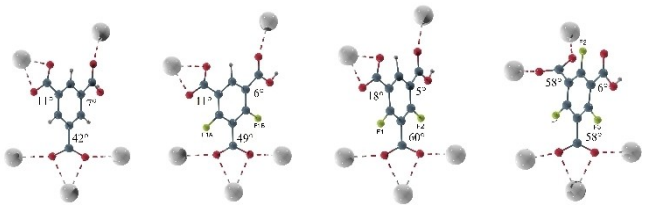

Figure 4. Coordination of $HBTC^{2-}$ linkers with different degrees of fluorination in the crystal structures of (from left to right) $^3_\infty$[Sr(H-BTC)$(H_2O)_2$]$\times\frac{1}{2}$ H_2O,[66] $^3_\infty$[Sr(H*mF*-BTC)$(H_2O)_2$]$\times\frac{1}{2}$ H_2O, $^3_\infty$[Sr(H*dF*-BTC)$(H_2O)_2$]$\times\frac{1}{2}$ H_2O, and $^2_\infty$[Sr(H*pF*-BTC)$(H_2O)_2$]×1.5 H_2O; Sr (large grey sphere), O (small red sphere), C (small dark blue sphere), F (small green sphere), and H (very small grey sphere).[68] Reprinted (adapted) with permission from ref. [68]. Copyright 2020 Wiley.

Table 2. Torsion angles between the phenyl ring and carboxylate moieties in selected coordination polymers (CPs) and MOFs with isostructural or at least isotopological networks. The mean value for each compound is given in brackets.

MOF/CP	BTC^{3-} Torsion angles/°	*mF*-BTC^{3-} Torsion angles/°	*dF*-BTC^{3-} Torsion angles/°	*pF*-BTC^{3-} Torsion angles/°
HKUST-1[2]→UHM-31[35]	5.5, 3× (5.5)	5.5, 3× (5.5)		
UHM-33[35]→*dF*-UHM-33[37]		12.8; 13.8; 47.3 (24.6)	11.7; 13.8; 47.9 (24.5)	
[Ba(*nF*-BTC)$(H_2O)_2$]$\times\frac{1}{2}$ H_2O[37]	7.3; 9.7; 37.8 (18.3)	6.5; 9.1; 44.8 (20.1)	5.7; 10.9; 51.6 (22.7)	
K(H_2*nF*-BTC)[37]		5.4; 24.5; 34.9 (21.6)	14.1; 15.5; 55.9 (28.5)	30.5; 48.9; 66.1 (48.5)
UoC-7(1F)→UoC-7(2F)[36]		5.2, 2×; 90 (33.5)	4.7, 2×; 90 (33.1)	
UoC-4[38]→UoC-6[39]			0; 90, 2× (60)	17.8; 81.4, 2× (60.2)
Mean value for all entries of a column	**11.9°**	**21.1°**	**33.8°**	**54.4°**

© 2025 The Author(s). European Journal of Inorganic Chemistry published by Wiley-VCH GmbH

10990682c, 2025, 10, Downloaded from https://chemistry-europe.onlinelibrary.wiley.com/doi/10.1002/ejic.202400809 by Bibl. der Universitat zu Koln, Wiley Online Library on [19/01/2026]. See the Terms and Conditions (https://onlinelibrary.wiley.com/terms-and-conditions) on Wiley Online Library for rules of use; OA articles are governed by the applicable Creative Commons License

ring were reported.[38] It should be noted that the two fluorine substituents are disordered over three positions in UoC-4. The coplanar arrangement is observed for the carboxylate group between two symmetry equivalent fluorine substituents which have the lowest site occupancy factor (F2, occ. = 59.3 %). For the carboxylate groups between F2 and F1 (occ. = 81.4 %), a perpendicular orientation with respect to the phenyl ring was reported.

With regard to the properties, two results on the CO_2 uptake are remarkable for fluorinated BTC-based MOFs. *Fröba* and coworkers reported a specific surface area $S_{BET} = 1802\ m^2/g$ for UHM-31 with the monofluorinated *mF*-BTC^{3-} linker,[35] which is significantly higher than reported for its non-fluorinated congener HKUST-1 with 692 m^2/g[2] in the original publication. However, in more recent articles, also S_{BET} values of 1333 m^2/g[70] or even 1944 m^2/g[71] were reported for this MOF. Possible reasons for these discrepancies will be discussed later on (chapter on MOFs with $BPTC^{4-}$ linkers). For UHM-31, it was found that the H_2 (+2.2 %) and the CH_4 uptake (+6.1 %) is only slightly affected by the fluorination of the linker, whereas the CO_2 uptake increases by almost 40 % for UHM-31 compared to HKUST-1.[35] A similar effect was found for UoC-7, an anionic bimetallic K–Zn MOF based on the mono- or the difluorinated BTC^{3-} linker.[36] For UoC-7(1F), a CO_2 uptake of 148 cm^3/g was measured at 293 K (1 bar). With a higher fluorination of the linker, the CO_2 uptake was increased by more than 10 % to 164 cm^3/g at 293 K and 1 bar in UoC-7(2F). The latter is one of the highest CO_2 uptakes at room temperature reported for a MOF to date.[36]

MOFs with $BPTC^{4-}$ Linkers and their Fluorinated Derivatives

Compared to the BDC^{2-} and the BTC^{3-} linkers discussed before, the $BPTC^{4-}$ linker exhibits a somewhat higher complexity. Not only the torsion between the carboxylate groups and the phenyl ring, but also the torsion between the two phenyl rings has to be considered. In MOF-505, Cu_2 paddlewheel units are combined with the $BPTC^{4-}$ linker to form a 3D MOF with almost spherical pores (Figure 5).[72] Three distinct steps for the activation were observed leading to an internal surface area $S_{Langmuir} = 1830\ m^2/g$. Both phenyl rings are coplanar ($\measuredangle C_{phenyl}$-$C_{phenyl} = 0°$) and a small torsion angle of 8.8° was found between the carboxylate group and the phenyl ring (all carboxylate groups are symmetrically equivalent).

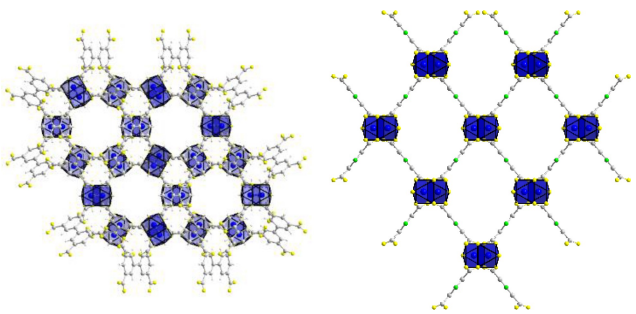

Figure 5. Excerpts of the crystal structures of MOF-505 (left, along [001]) and UoC-1 (right, along [100]); Cu (blue spheres), F (green spheres), O (yellow spheres), C (grey spheres), H (small white spheres), CuO_5 polyhedra are emphasized in blue.

With the mono- and difluorinated linkers *mF*-$BPTC^{4-}$ and *dF*-$BPTC^{4-}$, another class of MOFs was synthesized, named UoC-1(1F) and UoC-1(2F).[42] Only for UoC-1(1F), a single crystal structure analysis was reported so that reliable structural parameters can solely be given for this compound. Both phenyl rings are coplanar, however the torsion angle between the carboxylate group and the phenyl ring is increased to 28.7°. Again, all carboxylate groups are symmetrically equivalent and the fluorine substituent is disordered over two positions. Internal surfaces areas $S_{BET} = 1256\ m^2/g$ (UoC-1(1F)) and $S_{BET} = 1162\ m^2/g$ (UoC-1(2F)) were determined. Both MOF-505 ($R\bar{3}m$) and UoC-1 (*Imma*) were described in the NbO topology, however with a completely different symmetry. This leads to differing orientations of the Cu_2 paddlewheel units and thus different shapes of the pores, what can be traced back to the different torsion angles between the phenyl rings and the carboxylate moieties in both compounds. This is pictured in Figure 5.

The $BPTC^{4-}$ linker is best known from its incorporation into the MOFs of the MFM-300 family, sometimes denoted as NOTT-300 (with Al^{3+} nodes),[73] NOTT-400 (with Sc^{3+} nodes)[40] or InOF-1 (with In^{3+} nodes).[41] They are of particular interest due to their high chemical and thermal stability.[74–77] Also a derivative crystallizing in the same structure type with fluorine substituted $BPTC^{4-}$ has been published very recently, denoted as UoC-2.[43] A mono- as well as a difluorinated linker was incorporated. Fluorine substituents were introduced in the position between the two carboxylate groups of one phenyl ring (Scheme 1); in the MOFs with the monofluorinated linker (*mF*-$BPTC^{4-}$), this fluorine group is disordered over the two positions with an occupancy of 0.5 each. Examining the torsion angles between the two phenyl rings reveals that they are mainly unaffected by the introduction of fluorine substituents ranging from 31.1° in MFM-300(Ga)[78] to 33.8° for UoC-2(Ga,1F).[43] Surprisingly, also the torsion angles between the phenyl rings and the carboxylate groups – all carboxylate groups are crystallographically equivalent – show only a relatively small spread from 24.6° for MFM-300(In)[79] (27.7° in MFM-300(Ga)) to 30.6° for UoC-2(In,2F), 28.1° for UoC-2(Ga,1F) and 29.2° for UoC-2(In,1F). There is some dependence on a fluorine substituent in *ortho* position to a carboxylate group, but it remains small. From that point, it is not surprising that all compounds crystallize in the same crystal structure in space group $I4_122$.

With respect to properties, the thermal stability decreases with the introduction of fluorine substituents,[43] as was found for all CPs and MOFs discussed up to now. Figure 6 shows N_2 ad- and desorption isotherms of Ga-MOFs with the MFM-300 topology and an increasing number of fluorine substituents. S_{BET} increases from 1109 m^2/g (MFM-300(Ga)) to 1220 m^2/g (UoC-2(Ga,1F)) and 1310 m^2/g (UoC-2(2F,Ga)). These results are contrary to what was discussed before. In most cases up to now, the introduction of fluorine substituents led to a decrease of the internal surface area, which was attributed to the larger size of the fluorine atoms compared to hydrogen. However, the

© 2025 The Author(s). European Journal of Inorganic Chemistry published by Wiley-VCH GmbH

10990682c, 2025, 10, Downloaded from https://chemistry-europe.onlinelibrary.wiley.com/doi/10.1002/ejic.202400809 by Bibl. der Universitat zu Koln, Wiley Online Library on [19/01/2026]. See the Terms and Conditions (https://onlinelibrary.wiley.com/terms-and-conditions) on Wiley Online Library for rules of use; OA articles are governed by the applicable Creative Commons License

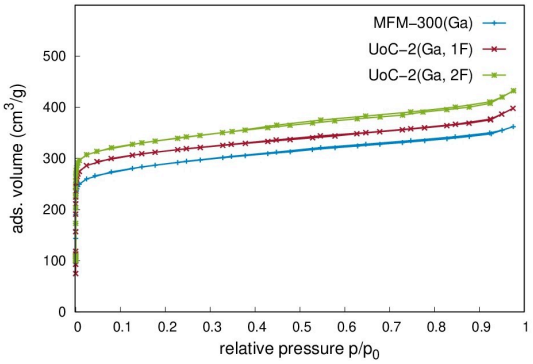

Figure 6. N_2 ad- and desorption isotherms of MFM-300(Ga) (blue curve), UoC-2(Ga,1F) (red curve) and UoC-2(Ga, 2F) (green curve). Reprinted (adapted) with permission from ref. [43]. Copyright 2024 Wiley.

BET extraction of these internal surfaces allows for a multilayer adsorption and thus, a higher S_{BET} might indicate a stronger interaction between the MOF host and the N_2 molecules up to a second (or even higher) layer. Indeed, it was shown in TGA experiments that there is a stronger interaction between solvent molecules and UoC-2 MOFs increasing with the number of fluorine substituents.[43] However, such a detailed discussion of S_{BET} values is always hampered by the low accuracy and reproducibility of such measurements. As was discussed for HKUST-1 (*vide supra*), the reported S_{BET} values range from 692 m^2/g[2] to 1944 m^2/g.[71] An incomplete release of solvent molecules upon activation, degradation of the framework upon heating during activation or a high number of local defects in the structure of the MOF framework were discussed as possible reasons for these effects.[80] This makes especially an optimized activation of FMOFs difficult, as the interaction of the solvent molecules with the MOF host increases with the number of fluorine substituents, whereas its thermal stability decreases. Therefore, the conditions for the activation have to be chosen very carefully.

Despite these drawbacks, FMOFs have shown some promising results with respect to CO_2 uptake (cp. UoC-7, *vide supra*).[36] For UoC-2(Ga,2F), a CO_2 uptake of 136 cm^3/g at 273 K (1 bar) was reported. This value is high, although it does not reach the uptake reported for UoC-7. The effect of fluorine substituents on the H_2 uptake is again almost negligible.[43]

MOFs with BTB^{3-} Linkers and their Fluorinated Derivatives

The BTB^{3-} linker is the most complex ligand discussed in this concept paper. Like in $BPTC^{4-}$, two different torsion angles have to be considered when elucidating its structural properties in the formation of MOFs and CPs: the angle between the carboxylate group and the outer phenyl ring (cp. Scheme 1) and the angle between the inner phenyl ring and the outer benzoate groups. Depending on the symmetry of the crystal structure, three independent angles of each of the two are possible. However in most cases, a higher symmetry leads to fewer independent angles. MOF-177[45] can be considered as a prototype MOF with the BTB^{3-} linker. Unfortunately, severe disorder in the reported crystal structures of MOF-177[45,81] hinders a reliable determination of the torsion angles discussed above. In Figure 7, the respective torsion angles of all entries of the MOF subset[19,20] of the CSD database[21] for MOFs containing the non-functionalized BTB^{3-} linker are presented in form of a heat map. There is obviously a maximum for the torsion angles between the inner phenyl rings and the outer benzoate groups of ~35 ° and the torsion angles between the outer phenyl rings and the carboxylate groups close to 0°.

Scheme 1 and Table 1 show that MOFs with a perfluorinated inner ring of the BTB^{3-} linker (denoted *3F*$_i$-BTB^{3-}) as well as partly (*3F*$_o$-BTB^{3-} and *6F*$_o$-BTB^{3-}) or perfluorinated outer rings (*12F*$_o$-BTB^{3-}) have been reported. MOFF-4 is the only example of a MOF with perfluorinated outer benzoate rings (*12F*$_o$-BTB^{3-}).[53] The linkers are connected via Cu_2 paddlewheel units forming a MOF with large cages of a diameter up to 33.5 Å. MOFF-4 is relatively unstable, decomposing at 220 °C and during activation so that only a small S_{BET} value of 510 m^2/g was measured pointing to a partial collapse of the MOF.[53] MOFF-4 shows some structural similarities with MOF-143, incorporating the unfluorinated BTB^{3-} linker.[82] However, a disorder of the perfluorinated benzoate rings within the *12F*$_o$-BTB^{3-} linker of MOFF-4 hinders a more detailed structural comparison. Torsion angles of 34.6° (between the inner and the benzoate rings) and 0.6° (between the outer ring and the carboxylate groups) have been determined in MOF-143,[82] in very good agreement with the hot spots shown in Figure 7. As mentioned, disorder hampers a structural comparison of MOF-177[45] with its fluorinated congeners MOF-177-H (with *3F*$_o$-BTB^{3-}) and MOF-177-F (with *6F*$_o$-BTB^{3-}).[51] For MOF-177-F, S_{BET} = 3690 m^2/g and $S_{Langmuir}$ = 4345 m^2/g were reported, which is a considerable decline compared to unfluorinated MOF-177 with S_{BET} = 4740 m^2/g and $S_{Langmuir}$ = 5340 m^2/g,[51] pointing to a lower spatial demand of hydrogen compared to fluorine. No gas sorption measurements were reported for MOF-177-H.

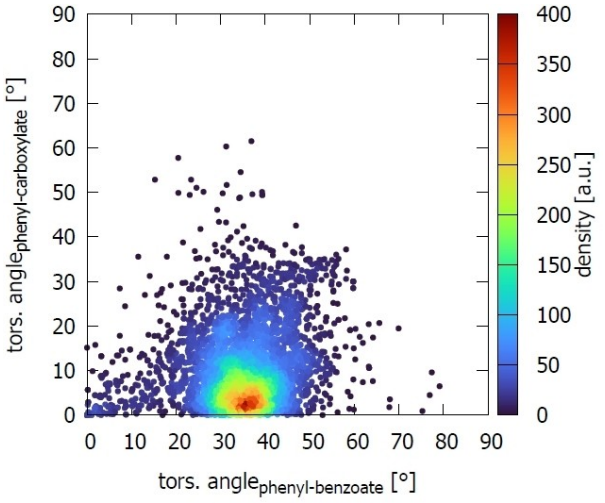

Figure 7. Plot of all torsion angles between the central ring and the benzoate ring against the torsion angles of the outer phenyl rings and their carboxylate groups found in MOFs with non-functionalized BTB^{3-} linkers (source: MOF subset[19,20] of the CSD database,[21] 431 entries).[85]

© 2025 The Author(s). European Journal of Inorganic Chemistry published by Wiley-VCH GmbH

10990682c, 2025, 10, Downloaded from https://chemistry-europe.onlinelibrary.wiley.com/doi/10.1002/ejic.202400809 by Bibl. der Universitat zu Koln, Wiley Online Library on [19/01/2026]. See the Terms and Conditions (https://onlinelibrary.wiley.com/terms-and-conditions) on Wiley Online Library for rules of use; OA articles are governed by the applicable Creative Commons License

Another interesting class of BTB-based MOFs are those with the MUV-12 topology. They are Ca/Ti based materials, which have been synthesized with the non-functionalized BTB^{3-} linker,[83] but also 3-fold substituted linkers, e.g. with fluorine substituents in *ortho* and *meta* position to the carboxylate moiety denominated *ortho*-$3F_o$-BTB^{3-} ($3F_o$-BTB^{3-} in Scheme 1) and *meta*-$3F_o$-BTB^{3-} (see footnote in Table 1).[52] Most important for the discussion in this work, no disorder of the phenyl rings or the carboxylate groups was found in the reported crystal structures so that the influence of the fluorine substituents in different positions of the outer benzoate rings on the resulting MOFs can be analysed reliably. All MUV-12 MOFs crystallize in space group $Im\bar{3}$ with a doubly interpenetrated framework isoreticular to MUV-10.[83] This shows that substituents in the outer benzoate rings obviously do not affect the structure formation significantly. In Table 3, some properties of the different MUV-12 materials are summarized.

The structural details, i.e. the torsion angles given in Table 3 corroborate the assumption that the fluorine substituents of the outer benzoate rings have only a minor influence on the conformation of the BTB^{3-} linker. The torsion angle between the inner phenyl ring and the outer benzoate rings range from 34.7° to 36.5° and are very close to the maximum (~35°) found in Figure 7 in a survey on 431 MOFs with non-functionalized BTB^{3-} linkers. The torsion angles between the outer phenyl rings and the carboxylate groups range from 11.4° to 23.9°. The highest torsion angle is, as expected, observed for the *ortho*-$3F_o$-BTB^{3-} linker with a fluorine substituent in *ortho* position to the carboxylate group. In Table 3, a third torsion angle is given, which is defined by the plane of the inner phenyl ring and the outer carboxylate groups. The resulting angles given in Table 3 show that the rotation between the inner ring and the benzoate ring is always compensated by an opposite rotation of the carboxylate groups, thus resulting in overall torsion angles in the range 12.5° to 25.1°. This leads to the somewhat unexpected observation that the smallest overall torsion angle is observed for the *ortho*-$3F_o$-BTB^{3-} linker. These compensating rotations are obviously the reason that the MUV-12 topology is also observed with many other substituents in the inner and the outer rings of the BTB^{3-} linkers.[52] The S_{BET} values given in Table 3 show that the fluorine substituents have no significant effect on the resulting surface areas. The thermal stability of MUV-12(*o*-F)$_3$ is decreased by ca. 50 °C compared to non-functionalized MUV-12 ($T_{dec} \approx 450$ °C), which is in line with the many examples discussed before. However, it is somewhat unexpected that with fluorine substituents in meta position to the carboxylate groups, i.e. in MUV-12(*m*-F)$_3$, no influence on the thermal stability compared to the non-functionalized MOF was observed.[52]

The results on MOFs of the MUV-12 family suggest that there is only a marginal influence of fluorine substituents in the outer rings of BTB^{3-} linkers on the structures of the resulting MOFs. UoC-3 is one of the very few examples of a MOF with a perfluorinated inner ring of the BTB^{3-} linker.[48] It forms large porous channels with a very high surface area (S_{BET} = 4844 m^2/g, cp. Table 3). Analogous to UoC-7, it exhibits an anionic framework with $(CH_3)_2NH_2^+$ cations counterbalancing its charge. It is based on UO_2^{2+} units and has a relatively high stability in water even under slightly acidic conditions. It turned out to be a very good cation exchanger for radioactive $^{137}Cs^+$ with a high K_d value of 4390(280) and good recyclability.[48] With the non-functionalized BTB^{3-} linker and the same UO_2^{2+} node, a 2D coordination polymer $[Me_2NH_2][UO_2(BTB)]\cdot DMF\cdot 6.5H_2O$ was reported, which also shows a very good applicability to remove radioactive $^{137}Cs^+$ from nuclear waste water.[84] In Table 3, the torsion angles in these two compounds are given. Apparently, the torsion angle between the inner ring and the outer benzoate rings increases significantly upon perfluorination of the inner ring: ∡(mean) = 48.2° for UoC-3 and ∡(mean) = 24.7° for $[Me_2NH_2][UO_2(BTB)]\cdot DMF\cdot 6.5H_2O$. Somewhat unexpected, the torsion angle between the outer ring and the carboxylate moiety also increases upon fluorination of the inner ring: ∡(mean) = 25.2° for UoC-3 and ∡(mean) = 13.8° for $[Me_2NH_2][UO_2(BTB)]\cdot DMF\cdot 6.5H_2O$. Current structural investigations of our group on further MOFs and CPs with the $3F_i$-BTB^{3-} linker as well as concomitant DFT calculations corroborate these findings.[85] Most likely, the high electron withdrawing nature of the fluorine substituents in the inner ring reduces the electron density even in the $C_{carboxylate}$-C_{phenyl} bonds of the outer ring so that the rotation barrier is reduced and thus allowing higher torsion angles between the carboxylates and the phenyl rings according to the spatial demands and repulsive interactions in the specific structure. In the discussion of the MOFs of the MUV-12 family, a third torsion angle between the plane of the carboxylate moieties and the inner ring was introduced. In $[Me_2NH_2][UO_2(BTB)]\cdot DMF\cdot 6.5H_2O$, the tilting between the inner ring and the benzoates is compensated by the rotation of the carboxylate group with respect to the outer ring. Thus, only

Table 3. Selected properties of some BTB-based MOFs.

MOF	Linker	S_{BET}	Torsion angle (carboxylate–outer phenyl ring)	Torsion angle (benzoate–inner phenyl ring)	Torsion angle (carboxylate–inner phenyl ring)
MUV-12[52]	BTB^{3-}	1590 m^2/g	16.7°	34.7°	17.5°
MUV-12(*o*-F)$_3$[52]	*ortho*-$3F_o$-BTB^{3-}[a]	1534 m^2/g	23.9°	36.2°	12.5°
MUV-12(*m*-F)$_3$[52]	*meta*-$3F_o$-BTB^{3-}[a]	1568 m^2/g	11.4°	36.5°	25.1°
UoC-3[48]	$3F_i$-BTB^{3-}	4844 m^2/g	27.4° (2×); 20.8°	40.3° (2×); 63.9°	12.9° (2×); 84.7°
$[Me_2NH_2][UO_2(BTB)]\cdot DMF\cdot 6.5H_2O$[84]	BTB^{3-}	n.d.	7.4°; 12.0°; 22.1°	22.6°; 24.7°; 26.7°	3.4°; 15.8°; 16.5°

[a] Fluorine substituents disordered over two positions.

© 2025 The Author(s). European Journal of Inorganic Chemistry published by Wiley-VCH GmbH

10990682c, 2025, 10, Downloaded from https://chemistry-europe.onlinelibrary.wiley.com/doi/10.1002/ejic.202400809 by Bibl. der Universitat zu Koln, Wiley Online Library on [19/01/2026]. See the Terms and Conditions (https://onlinelibrary.wiley.com/terms-and-conditions) on Wiley Online Library for rules of use; OA articles are governed by the applicable Creative Commons License

small torsion angles between the plane of the carboxylate moieties and the inner ring result, ranging from 3.4° to 16.5°. Accordingly, BTB^{3-} can be assumed as being almost planar (cp. Figure 8). In UoC-3, in one of the three benzoate substituents, the rotations do not compensate leading to an almost perpendicular arrangement of the outer carboxylate moiety with respect to the inner ring (84.7°). Evidently, this has a high impact on the resulting crystal structure leading to the 3D porous structure of UoC-3. These considerations are graphically summarized in Figure 8.

The structure directing influence of substituents in the inner ring of BTB^{3-} linkers can also be seen in the giant UO_2^{2+} based MOF NU-1301. Here, all hydrogen atoms of the inner ring of a BTB^{3-} linker are replaced by methyl groups, which leads to torsion angles between the inner ring and the outer benzoate rings of ~90°. This perpendicular arrangement of the phenyl rings within the linker leads to a 3D MOF exhibiting an unprecedented complexity with 816 uranyl nodes and linkers in the unit cell and a unit cell volume of 5,201,096 Å^3.[86]

Summary and Outlook

In this concept paper, the influence of fluorine substituents in aromatic carboxylate linkers on the (structural) properties of the resulting coordination polymers (CPs) and MOFs is analysed. The focus is on four well-known linkers that lead to the formation of a variety of MOFs/CPs, namely 1,4-benzenedicarboxylate (BDC^{2-}), 1,3,5-benzenetricarboxylate (BTC^{3-}), 3,3′,5,5′-biphenyltetracarboxylate ($BPTC^{4-}$), and 1,3,5-benzenetribenzoate (BTB^{3-}) as well as its fluorinated counterparts. It is a clear trend that with fluorine substituents in *ortho* position to the carboxylate group, the torsion angle between this carboxylate moiety and the phenyl ring is significantly increased. For BDC^{2-} linkers, this torsion can be compensated by a counter-rotation of the opposite carboxylate groups in *para* position, so that a variety of isostructural MOFs with fluorinated BDC^{2-} linkers has been reported (e.g. MIL-53, MIL-88, UiO-66).

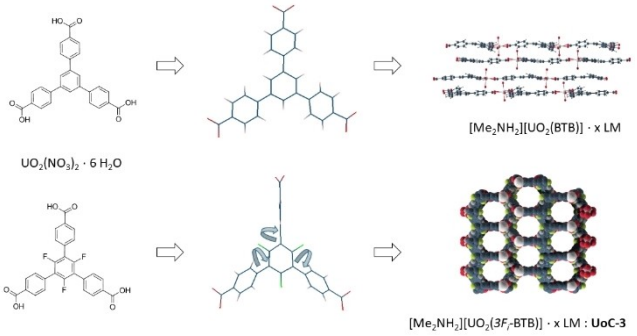

Figure 8. Top: formation of the 2D CP $[Me_2NH_2][UO_2(BTB)]\cdot DMF\cdot 6.5H_2O$[84] from a non-functionalized BTB^{3-} linker. Bottom: construction of the 3D MOF UoC-3[48] from a $3F_i$-BTB^{3-} linker and UO_2^{2+} nodes. The structure directing influence of the torsion angles between the inner phenyl ring and the outer benzoate groups is emphasized by arrows. The wireframe pictures of the linkers in the middle represent its geometric arrangement as found in the respective MOF/CP.

This compensating rotation is not possible for BTC^{3-} based linkers with carboxylate groups in 1,3,5 positions. Here, isostructural MOFs are only found for linkers with a low number of fluorine substituents (e.g. HKUST-1 and UHM-31 with the monofluorinated *mF*-BTC^{3-} linker), as the influence of only one fluorine substituents on the torsion angles remains small.

For $BPTC^{4-}$ and BTB^{3-} type linkers, the interplanar angle between two phenyl rings has to be considered as a second structure directing property. For MOFs with $BPTC^{4-}$ type linkers, only examples with a mono- and a disubstituted linker were reported. Here, the influence on the torsion angles is small and several isostructural MOFs with MFM-300 topology were synthesized. The situation is more complex for MOFs with the BTB^{3-} linker. Fluorine substituents can be incorporated in both the inner and the outer benzoate ring. In several examples reported in the literature, the influence of fluorine substituents in the outer benzoate rings of the BTB^{3-} linkers is almost negligible. Accordingly, some isostructural MOFs have been reported (e.g. MUV-12). One of the very few examples of a MOF with a perfluorination of the inner ring is UoC-3. Here, the fluorination leads to a completely different structure (a 3D MOF with large porous channels) compared to the compound obtained with a non-functionalized BTB^{3-} linker (a 2D CP, cp. Figure for Table of Content). It is therefore one of the central goals of our research to synthesize further examples of MOFs with the $3F_i$-BTB^{3-} linker.

With regard to properties, two results were clearly identified in this concept paper:

a) Fluorine substituents decrease the thermal stability of the resulting MOFs. However, this influence depends very much on the position of the fluorine atom with respect to the carboxylate moiety. Substituents in *ortho* positions have the strongest effect.
b) Gas sorption is typically enhanced by fluorine substituents due to stronger interactions between the guest molecules and the MOF host. This effect depends very much on the electron count of the guest, e.g. it is much stronger for CO_2 than for H_2. This suggests a *van der Waals* type interaction between the guest and the host. Based on that, one may predict very interesting gas sorption properties for sulphur containing gases, which makes these MOFs interesting candidates for gas purification.

In this concept paper, the specific requirements for a successful synthesis of FMOFs have not been addressed up to now. The increased acidity of the acids of the partly fluorinated/perfluorinated linkers may need some adjustments in the synthetic protocols compared to the synthesis with non-fluorinated linkers. Differing solubilities of starting materials and products can make the use of other solvents necessary. In our experience, DMA (*N*,*N*-dimethylacetamide) is very often a good choice.

At the moment, the conclusions drawn in this concept paper, are mainly based on the analysis of published compounds. To support them, our group has started to conduct DFT calculations on the linkers as well as structural fragments of the resulting MOFs. Basically, these calculations corroborate the conclusions drawn in this concept paper.[85] An interesting "by-

© 2025 The Author(s). European Journal of Inorganic Chemistry published by Wiley-VCH GmbH

10990682c, 2025, 10, Downloaded from https://chemistry-europe.onlinelibrary.wiley.com/doi/10.1002/ejic.202400809 by Bibl. der Universitat zu Koln, Wiley Online Library on [19/01/2026]. See the Terms and Conditions (https://onlinelibrary.wiley.com/terms-and-conditions) on Wiley Online Library for rules of use; OA articles are governed by the applicable Creative Commons License

product" of these calculations is the finding that the electrostatic potential of the inner ring of $3F_i$-BTB^{3-} is completely inverted leading to a highly positive charge distribution in the inner ring.[85] This explains some very recent findings of guest inclusion in UoC-9, a Ca-based MOF with the $3F_i$-BTB^{3-} linker.[87]

In 2023, *Yaghi* and co-workers presented a GPT-4 based approach for the synthesis of new MOFs.[88] Using this method, they synthesized the Al-based MOF-521 with different BTB^{3-} linkers and additional formate anions. Isostructural compounds were obtained with the non-functionalized BTB^{3-}, the *ortho*-$3F_o$-BTB^{3-}, and the *meta*-$3F_o$-BTB^{3-} linkers. Are these results contradictory to the analysis in this concept paper? No, they are not! The torsion angles between the inner ring and the benzoate rings show the following trend: 62.9° (BTB^{3-}), 51.9° (*ortho*-$3F_o$-BTB^{3-}), and 68.0° (*meta*-$3F_o$-BTB^{3-}), whereas for the torsion angles between the outer benzoate rings and the carboxylate groups these values were determined: 28.7° (BTB^{3-}), 37.2° (*ortho*-$3F_o$-BTB^{3-}), and 22.8° (*meta*-$3F_o$-BTB^{3-}). These results are more or less in line with the expected results and those obtained for MOFs of the MUV-12 family. However, it is very remarkable that all torsion angles add up to a total value for the torsion between the inner ring and the outer carboxylate group of 90°, i.e. these groups are perpendicular to each other in all MOF-521 structures.

Acknowledgements

I would like to thank all my co-workers that contributed with their research results to the topic of this concept paper. My special thanks go to the current members of the "MOF subgroup" (A. E. L. Cammiade, R. K. Christoffels, T. Mattick, S. S. Sebastian, J. P. Weber) for proofreading, numerous discussions and providing illustrations. Funding by the Deutsche Forschungsgemeinschaft (DFG, Project No. RU 546/12-1 and RU 546/16-1) is gratefully acknowledged. Open Access funding enabled and organized by Projekt DEAL.

Conflict of Interests

The author declares no conflict of interest.

Data Availability Statement

The data that support the findings of this study are available from the corresponding author upon reasonable request.

Keywords: aromatic carboxylates · fluorinated linker · isostructural · MOF · torsion angle

[1] H. Li, M. Eddaoudi, M. O'Keeffe, O. M. Yaghi, *Nature* **1999**, *402*, 276–279.
[2] S. S.-Y. Chui, S. M.-F. Lo, J. P. H. Charmant, A. G. Orpen, I. D. Williams, *Science* **1999**, *283*, 1148–1150.
[3] O. M. Yaghi, G. Li, H. Li, *Nature* **1995**, *378*, 703–706.
[4] M. Kondo, T. Yoshitomi, H. Matsuzaka, S. Kitagawa, K. Seki, *Angew. Chem. Int. Ed.* **1997**, *36*, 1725–1727.
[5] S. Subramanian, M. J. Zaworotko, *Angew. Chem. Int. Ed.* **1995**, *34*, 2127–2129.
[6] B. F. Hoskins, R. Robson, *J. Am. Chem. Soc.* **1990**, *112*, 1546–1554.
[7] C. Yang, X. Wang, M. A. Omary, *J. Am. Chem. Soc.* **2007**, *129*, 15454–15455.
[8] S. Kumar, B. Mohan, C. Fu, V. Gupta, P. Ren, *Coord. Chem. Rev.* **2023**, *476*, 214876.
[9] A. Ebadi Amooghin, H. Sanaeepur, R. Luque, H. Garcia, B. Chen, *Chem. Soc. Rev.* **2022**, *51*, 7427–7508.
[10] R. A. Fischer, C. Wöll, *Angew. Chem. Int. Ed.* **2008**, *47*, 8164–8168.
[11] C. Serre, *Angew. Chem. Int. Ed.* **2012**, *51*, 6048–6050.
[12] Z. Zhang, O. Š. Miljanić, *Org. Mater.* **2019**, *1*, 19–29.
[13] S. Noro, T. Nakamura, *NPG Asia Mater.* **2017**, *9*, e433–e433.
[14] D. Morelli Venturi, F. Costantino, *RSC Adv.* **2023**, *13*, 29215–29230.
[15] P. Pachfule, Y. Chen, J. Jiang, R. Banerjee, *Chem. Eur. J.* **2012**, *18*, 688–694.
[16] S. Surblé, C. Serre, C. Mellot-Draznieks, F. Millange, G. Férey, *Chem. Commun.* **2006**, 284–286.
[17] T.-H. Chen, I. Popov, O. Zenasni, O. Daugulis, O. Š. Miljanić, *Chem. Commun.* **2013**, *49*, 6846–6848.
[18] H. Furukawa, J. Kim, N. W. Ockwig, M. O'Keeffe, O. M. Yaghi, *J. Am. Chem. Soc.* **2008**, *130*, 11650–11661.
[19] P. Z. Moghadam, A. Li, S. B. Wiggin, A. Tao, A. G. P. Maloney, P. A. Wood, S. C. Ward, D. Fairen-Jimenez, *Chem. Mater.* **2017**, *29*, 2618–2625.
[20] P. Z. Moghadam, A. Li, X.-W. Liu, R. Bueno-Perez, S.-D. Wang, S. B. Wiggin, P. A. Wood, D. Fairen-Jimenez, *Chem. Sci.* **2020**, *11*, 8373–8387.
[21] C. R. Groom, I. J. Bruno, M. P. Lightfoot, S. C. Ward, *Acta Crystallogr., B: Struct. Sci., Cryst. Eng. Mater.* **2016**, *72*, 171–179.
[22] K. Seki, S. Takamizawa, W. Mori, *Chem. Lett.* **2001**, *30*, 332–333.
[23] T. Loiseau, C. Serre, C. Huguenard, G. Fink, F. Taulelle, M. Henry, T. Bataille, G. Férey, *Chem. Eur. J.* **2004**, *10*, 1373–1382.
[24] G. Férey, C. Mellot-Draznieks, C. Serre, F. Millange, J. Dutour, S. Surblé, I. Margiolaki, *Science* **2005**, *309*, 2040–2042.
[25] J. H. Cavka, S. Jakobsen, U. Olsbye, N. Guillou, C. Lamberti, S. Bordiga, K. P. Lillerud, *J. Am. Chem. Soc.* **2008**, *130*, 13850–13851.
[26] H. Yang, T. X. Trieu, X. Zhao, Y. Wang, Y. Wang, P. Feng, X. Bu, *Angew. Chem. Int. Ed.* **2019**, *58*, 11757–11762.
[27] R. Matsuda, W. Kosaka, R. Kitaura, Y. Kubota, M. Takata, S. Kitagawa, *Microporous Mesoporous Mater.* **2014**, *189*, 83–90.
[28] C. Xiong, Y.-H. Xiao, Q. Liu, L. Chen, C.-T. He, Q.-Y. Liu, Y.-L. Wang, *Inorg. Chem. Front.* **2022**, *9*, 5064–5071.
[29] D. Morelli Venturi, V. Guiotto, R. D'Amato, L. Calucci, M. Signorile, M. Taddei, V. Crocellà, F. Costantino, *Mol. Syst. Des. Eng.* **2023**, *8*, 586–590.
[30] P. Horcajada, F. Salles, S. Wuttke, T. Devic, D. Heurtaux, G. Maurin, A. Vimont, M. Daturi, O. David, E. Magnier, N. Stock, Y. Filinchuk, D. Popov, C. Riekel, G. Férey, C. Serre, *J. Am. Chem. Soc.* **2011**, *133*, 17839–17847.
[31] Z. Chen, X. Wang, H. Noh, G. Ayoub, G. W. Peterson, C. T. Buru, T. Islamoglu, O. K. Farha, *CrystEngComm* **2019**, *21*, 2409–2415.
[32] M. D. DeFuria, M. Zeller, D. T. Genna, *Cryst. Growth Des.* **2016**, *16*, 3530–3534.
[33] T. Loiseau, L. Lecroq, C. Volkringer, J. Marrot, G. Férey, M. Haouas, F. Taulelle, S. Bourrelly, P. L. Llewellyn, M. Latroche, *J. Am. Chem. Soc.* **2006**, *128*, 10223–10230.
[34] C. Volkringer, D. Popov, T. Loiseau, G. Férey, M. Burghammer, C. Riekel, M. Haouas, F. Taulelle, *Chem. Mater.* **2009**, *21*, 5695–5697.
[35] K. Peikert, F. Hoffmann, M. Fröba, *CrystEngComm* **2015**, *17*, 353–360.
[36] S. Wenzel, A. E. L. Cammiade, R. K. Christoffels, S. S. Sebastian, T. Mattick, U. Ruschewitz, *Chem. Eur. J.* **2024**, *30*, e202400445.
[37] J. Krautwurst, D. Smets, R. Lamann, U. Ruschewitz, *Inorg. Chem.* **2019**, *58*, 8622–8632.
[38] T. Mattick, D. Smets, R. Christoffels, L. Körtgen, C. Tobeck, U. Ruschewitz, *Z. Anorg. Allg. Chem.* **2020**, *647*, 490–495.
[39] J. Krautwurst, R. Lamann, U. Ruschewitz, *Z. Naturforsch. B* **2021**, *76*, 849–856.
[40] I. A. Ibarra, S. Yang, X. Lin, A. J. Blake, P. J. Rizkallah, H. Nowell, D. R. Allan, N. R. Champness, P. Hubberstey, M. Schröder, *Chem. Commun.* **2011**, *47*, 8304–8306.
[41] R. A. Peralta, B. Alcántar-Vázquez, M. Sánchez-Serratos, E. González-Zamora, I. A. Ibarra, *Inorg. Chem. Front.* **2015**, *2*, 898–903.
[42] C. Stastny, U. Ruschewitz, *Z. Anorg. Allg. Chem.* **2018**, *644*, 1908–1914.
[43] C. Breitenbach (née Stastny), R. Christoffels, T. Mattick, A. Edelmann, T. Pierkes, S. König, M. Fröba, U. Ruschewitz, *Eur. J. Inorg. Chem.* **2024**, *27*, e202400231.

© 2025 The Author(s). European Journal of Inorganic Chemistry published by Wiley-VCH GmbH

10990682c, 2025, 10, Downloaded from https://chemistry-europe.onlinelibrary.wiley.com/doi/10.1002/ejic.202400809 by Bibl. der Universitat zu Koln, Wiley Online Library on [19/01/2026]. See the Terms and Conditions (https://onlinelibrary.wiley.com/terms-and-conditions) on Wiley Online Library for rules of use; OA articles are governed by the applicable Creative Commons License

[44] J. Duan, M. Higuchi, S. Horike, M. L. Foo, K. P. Rao, Y. Inubushi, T. Fukushima, S. Kitagawa, *Adv. Funct. Mater.* **2013**, *23*, 3525–3530.
[45] H. K. Chae, D. Y. Siberio-Pérez, J. Kim, Y. Go, M. Eddaoudi, A. J. Matzger, M. O'Keeffe, O. M. Yaghi, *Nature* **2004**, *427*, 523–527.
[46] S. Lee, E. A. Kapustin, O. M. Yaghi, *Science* **2016**, *353*, 808–811.
[47] H. Wang, X. Pei, D. M. Proserpio, O. M. Yaghi, *Isr. J. Chem.* **2021**, *61*, 774–781.
[48] R. Christoffels, C. Breitenbach (nee Stastny), J. Weber, L. Körtgen, C. Tobeck, M. Wilhelm, S. Mathur, J.-M. Neudörfl, M. Farid, M. Maslo, E. Strub, U. Ruschewitz, *Cryst. Growth Des.* **2022**, *22*, 681–692.
[49] S. S. Sebastian, F. P. Dicke, U. Ruschewitz, *Dalton Trans.* **2023**, *52*, 5926–5934.
[50] U. Ruschewitz, S. S. Sebastian, F. P. Dicke, *Z. Anorg. Allg. Chem.* **2024**, *650*, e202400089.
[51] Y.-B. Zhang, H. Furukawa, N. Ko, W. Nie, H. J. Park, S. Okajima, K. E. Cordova, H. Deng, J. Kim, O. M. Yaghi, *J. Am. Chem. Soc.* **2015**, *137*, 2641–2650.
[52] N. M. Padial, C. Chinchilla-Garzón, N. Almora-Barrios, J. Castells-Gil, J. González-Platas, S. Tatay, C. Martí-Gastaldo, *J. Am. Chem. Soc.* **2023**, *145*, 21397–21407.
[53] T. Chen, I. Popov, W. Kaveevivitchai, Y. Chuang, Y. Chen, A. J. Jacobson, O. Š. Miljanić, *Angew. Chem. Int. Ed.* **2015**, *54*, 13902–13906.
[54] A. Orthaber, C. Seidel, F. Belaj, J. H. Albering, R. Pietschnig, U. Ruschewitz, *Inorg. Chem.* **2010**, *49*, 9350–9357.
[55] C. Seidel, R. Ahlers, U. Ruschewitz, *Cryst. Growth Des.* **2011**, *11*, 5053–5063.
[56] Z. Hulvey, J. D. Furman, S. A. Turner, M. Tang, A. K. Cheetham, *Cryst. Growth Des.* **2010**, *10*, 2041–2043.
[57] Z. Wang, V. C. Kravtsov, R. B. Walsh, M. J. Zaworotko, *Cryst. Growth Des.* **2007**, *7*, 1154–1162.
[58] L.-M. Yang, G.-Y. Fang, J. Ma, R. Pushpa, E. Ganz, *Phys. Chem. Chem. Phys.* **2016**, *18*, 32319–32330.
[59] H. Zhang, F. Xiao, H. Han, Y. Wu, *J. Membr. Sci.* **2025**, *713*, 123261.
[60] J. H. Yoon, S. B. Choi, Y. J. Oh, M. J. Seo, Y. H. Jhon, T. B. Lee, D. Kim, S. H. Choi, J. Kim, *Catal. Today* **2007**, *120*, 324–329.
[61] D. Bara, E. G. Meekel, I. Pakamorė, C. Wilson, S. Ling, R. S. Forgan, *Mater. Horiz.* **2021**, *8*, 3377–3386.
[62] Z. Hu, Y. Peng, Z. Kang, Y. Qian, D. Zhao, *Inorg. Chem.* **2015**, *54*, 4862–4868.
[63] M. L. Díaz-Ramírez, E. Sánchez-González, J. R. Álvarez, G. A. González-Martínez, S. Horike, K. Kadota, K. Sumida, E. González-Zamora, M.-A. Springuel-Huet, A. Gutiérrez-Alejandre, V. Jancik, S. Furukawa, S. Kitagawa, I. A. Ibarra, E. Lima, *J. Mater. Chem. A* **2019**, *7*, 15101–15112.
[64] M. Eddaoudi, J. Kim, N. Rosi, D. Vodak, J. Wachter, M. O'Keeffe, O. M. Yaghi, *Science* **2002**, *295*, 469–472.
[65] D. J. Tranchemontagne, J. R. Hunt, O. M. Yaghi, *Tetrahedron* **2008**, *64*, 8553–8557.
[66] F. Micheel, W. Busse, *Chem. Ber.* **1957**, *90*, 2049–2053.
[67] J. Krautwurst, R. Lamann, U. Ruschewitz, *Z. Anorg. Allg. Chem.* **2017**, *643*, 1397–1405.
[68] D. Smets, U. Ruschewitz, *Z. Anorg. Allg. Chem.* **2020**, *646*, 1157–1167.
[69] M. J. Plater, A. J. Roberts, J. Marr, E. E. Lachowski, R. A. Howie, *Dalton Trans.* **1998**, 797–802.
[70] Q. Min Wang, D. Shen, M. Bülow, M. Ling Lau, S. Deng, F. R. Fitch, N. O. Lemcoff, J. Semanscin, *Microporous Mesoporous Mater.* **2002**, *55*, 217–230.
[71] A. G. Wong-Foy, A. J. Matzger, O. M. Yaghi, *J. Am. Chem. Soc.* **2006**, *128*, 3494–3495.
[72] B. Chen, N. W. Ockwig, A. R. Millward, D. S. Contreras, O. M. Yaghi, *Angew. Chem. Int. Ed.* **2005**, *44*, 4745–4749.
[73] S. Yang, J. Sun, A. J. Ramirez-Cuesta, S. K. Callear, W. I. F. David, D. P. Anderson, R. Newby, A. J. Blake, J. E. Parker, C. C. Tang, M. Schröder, *Nat. Chem.* **2012**, *4*, 887–894.
[74] J. H. Carter, C. G. Morris, H. G. W. Godfrey, S. J. Day, J. Potter, S. P. Thompson, C. C. Tang, S. Yang, M. Schröder, *ACS Appl. Mater. Interfaces* **2020**, *12*, 42949–42954.
[75] X. Han, H. G. W. Godfrey, L. Briggs, A. J. Davies, Y. Cheng, L. L. Daemen, A. M. Sheveleva, F. Tuna, E. J. L. McInnes, J. Sun, C. Drathen, M. W. George, A. J. Ramirez-Cuesta, K. M. Thomas, S. Yang, M. Schröder, *Nat. Mater.* **2018**, *17*, 691–696.
[76] X. Han, W. Lu, Y. Chen, I. da Silva, J. Li, L. Lin, W. Li, A. M. Sheveleva, H. G. W. Godfrey, Z. Lu, F. Tuna, E. J. L. McInnes, Y. Cheng, L. L. Daemen, L. J. M. MPherson, S. J. Teat, M. D. Frogley, S. Rudić, P. Manuel, A. J. Ramirez-Cuesta, S. Yang, M. Schröder, *J. Am. Chem. Soc.* **2021**, *143*, 3153–3161.
[77] J. A. Zárate, E. Sánchez-González, D. R. Williams, E. González-Zamora, V. Martis, A. Martínez, J. Balmaseda, G. Maurin, I. A. Ibarra, *J. Mater. Chem. A* **2019**, *7*, 15580–15584.
[78] C. P. Krap, R. Newby, A. Dhakshinamoorthy, H. García, I. Cebula, T. L. Easun, M. Savage, J. E. Eyley, S. Gao, A. J. Blake, W. Lewis, P. H. Beton, M. R. Warren, D. R. Allan, M. D. Frogley, C. C. Tang, G. Cinque, S. Yang, M. Schröder, *Inorg. Chem.* **2016**, *55*, 1076–1088.
[79] J. Qian, F. Jiang, D. Yuan, M. Wu, S. Zhang, L. Zhang, M. Hong, *Chem. Commun.* **2012**, *48*, 9696–9698.
[80] M. Agrawal, R. Han, D. Herath, D. S. Sholl, *Proc. Natl. Acad. Sci. USA* **2020**, *117*, 877–882.
[81] Y. Feng, T. Wang, Y. Li, J. Li, J. Wu, B. Wu, L. Jiang, C. Wang, *J. Am. Chem. Soc.* **2015**, *137*, 15055–15060.
[82] H. Furukawa, Y. B. Go, N. Ko, Y. K. Park, F. J. Uribe-Romo, J. Kim, M. O'Keeffe, O. M. Yaghi, *Inorg. Chem.* **2011**, *50*, 9147–9152.
[83] E. López-Maya, N. M. Padial, J. Castells-Gil, C. R. Ganivet, A. Rubio-Gaspar, F. G. Cirujano, N. Almora-Barrios, S. Tatay, S. Navalón, C. Martí-Gastaldo, *Angew. Chem. Int. Ed.* **2021**, *60*, 11868–11873.
[84] Y. Wang, Z. Liu, Y. Li, Z. Bai, W. Liu, Y. Wang, X. Xu, C. Xiao, D. Sheng, J. Diwu, J. Su, Z. Chai, T. E. Albrecht-Schmitt, S. Wang, *J. Am. Chem. Soc.* **2015**, *137*, 6144–6147.
[85] Sean S. Sebastian, *Novel MOFs Based on Fluorinated Aromatic Carboxylate-Ligands and Analysis of Host-Guest-Interactions in Their Pores, PhD Thesis*, University of Cologne, **2024**, p. 156.
[86] P. Li, N. A. Vermeulen, C. D. Malliakas, D. A. Gómez-Gualdrón, A. J. Howarth, B. L. Mehdi, A. Dohnalkova, N. D. Browning, M. O'Keeffe, O. K. Farha, *Science* **2017**, *356*, 624–627.
[87] S. S. Sebastian, F. P. Dicke, U. Ruschewitz, *CrystEngComm* **2024**, *26*, 6361–6368.
[88] Z. Zheng, Z. Rong, N. Rampal, C. Borgs, J. T. Chayes, O. M. Yaghi, *Angew. Chem. Int. Ed.* **2023**, *62*, e202311983.

Manuscript received: December 8, 2024
Revised manuscript received: February 11, 2025
Accepted manuscript online: February 14, 2025
Version of record online: February 25, 2025

© 2025 The Author(s). European Journal of Inorganic Chemistry published by Wiley-VCH GmbH

10990682c, 2025, 10, Downloaded from https://chemistry-europe.onlinelibrary.wiley.com/doi/10.1002/ejic.202400809 by Bibl. der Universitat zu Koln, Wiley Online Library on [19/01/2026]. See the Terms and Conditions (https://onlinelibrary.wiley.com/terms-and-conditions) on Wiley Online Library for rules of use; OA articles are governed by the applicable Creative Commons License